ELSEVIER

Journal of Nuclear Materials 275 (1999) 287–295

journal of nuclear materials

www.elsevier.nl/locate/jnucmat

A thermodynamic database for zirconium alloys

N. Dupin[a], I. Ansara[a], C. Servant[b], C. Toffolon[d], C. Lemaignan[c,*], J.C. Brachet[d]

[a] *Laboratoire de Thermodynamique et de Physico-Métallurgiques, E.N.S.E.E.G., BP 75, 38402 St. Martin d'Hères, France*
[b] *Laboratoire de Métallurgie Structurale, URA CNRS 1107, Université de Paris-Sud, 91405 Orsay, France*
[c] *Commissariat à l'Énergie Atomique, CEA-Grenoble DEC, 17 Rue des Martyrs, 38054 Grenoble, cedex 9, France*
[d] *Commissariat à l'Énergie Atomique, Saclay, CEREM/SRMA, 91991 Gif s/Yvette, France*

Received 2 February 1999; accepted 20 May 1999

Abstract

A thermodynamic database, Zircobase, was developed for zirconium alloys for use in the nuclear industry. Two examples of the assessments concerning the Sn–Zr and H–Zr systems are given. The complete set for the binary systems, compiled or assessed during the course of this study, is to be found on the web site: www.inpg.fr/ltpcm/base/zircobase. The utility of this database is demonstrated in examples of thermodynamic calculations of the α/β phase transformation temperatures performed on industrial Zr–Nb and Zy4 type alloys. These last results show fairly good predictions, using extrapolations of the actual thermodynamic database to ternary or higher order systems.

1. Introduction

Zirconium alloys are mainly used in nuclear industry for structural parts in the core as pressure tubes, channels, guide tubes or fuel cladding. The need for better efficiency of the nuclear industry is a driving force for the improvement of the properties of the alloys used, i.e. corrosion resistance and mechanical behaviour. This can be obtained either by a better control of the microstructure during advanced heat treatments or development of new alloys [1,2].

While zirconium alloys are used since several decades, a basic understanding of their metallurgy is still weak. Indeed, the very low solubility of transition metals in Zr, in connection with the high affinity of oxygen and hydrogen, leads to difficulties in obtaining 'pure' alloys. Thus a set of self-consistent thermodynamical databases that would help for a better understanding of the phases obtained during thermo-mechanical processing of known Zr alloys, as well as for the development of new alloys, is desirable in forecasting the phases to be expected and their stabilities [3].

In the framework of a co-operation between the French nuclear industry and research institutions, a thermodynamic database for Zr alloys has been developed. Based on a critical review of the data currently available. The Calphad approach, which has already been applied to other classes of alloys, has been used to evaluate the thermodynamic properties of the phases existing in the systems.

At this stage, the database is limited to the description of the following binary systems required for the study of higher order systems (ternary, *n*-aries): Zr–(Nb, Sn, O, H, Fe, Cr, Ni, V), Nb–(Sn, O, H, Fe, Cr), Sn–(O, Fe).

The aim of this paper is to present the procedure and the different models used for the set-up of this 'Zircobase', with emphasis on two selected systems of particular interest. The rest of the data can be listed from the web site: www.inpg.fr/ltpcm/base/zircobase.

2. Thermodynamic modelling

The calculation of phase equilibria implies the knowledge of the Gibbs energies of formation of all the

* Corresponding author. Tel.: +33-4 76 88 44 71; fax: +33-4 76 88 51 51.
E-mail address: lemaignan@cea.fr (C. Lemaignan)

0022-3115/99/$ - see front matter
PII: S0022-3115(99)00125-7

phases present in the system. For a database describing the thermodynamic behaviour of a multicomponent system, information relative to each sub-system (unary, binary,...) has to be introduced. The thermodynamic parameters are derived from an optimisation procedure which takes into account all the existing experimental results, such as phase diagram information, calorimetric, emf or vapour pressure results. Their meaning and the models using them are presented hereunder.

2.1. Pure elements

The Gibbs energy of an element, in a given physical state φ. $G_i^{\circ,\varphi}(T)$, at a given temperature T and pressure P, referred to the enthalpy of that element in its stable physical state at 298.15 K, $H_i^{\circ,\mathrm{SER}}$ (298.15 K), is expressed by

$$G_i^{\circ,\varphi}(T) - H_i^{\circ,\mathrm{SER}}(298.15\ \mathrm{K}) = a + bT + cT\ \ln\ T + \sum_n d_n T^n, \tag{1}$$

where n takes the value $2, 3, -1, \ldots$

The thermodynamic functions for the stable and metastable states are taken from the Scientific Group Thermodata Europe (SGTE) [4].

2.2. Stoichiometric compounds

The Gibbs energy of formation of a stoichiometric compound, C, is equal to

$$G_{\mathrm{C}}^{\circ}(T) - \sum_i a_i G_i^{\circ,\mathrm{SER}}(T) = a + bT + cT\ \ln\ T, \tag{2}$$

where a_i is the stoichiometric coefficient of the element i in C.

2.3. Substitutional solutions

For a binary system A–B, the Gibbs energy of a substitutional solution, φ, is expressed by the following equation:

$$G_m^{\varphi} - \sum_{i=\mathrm{A,B}} x_i^{\varphi} H_i^{\circ,\mathrm{SER}}(298.15\ \mathrm{K}) = G^{\mathrm{ref},\varphi} + G^{\mathrm{id},\varphi} + G^{\mathrm{xs},\varphi} \tag{3}$$

with

$$G^{\mathrm{ref},\varphi} = \sum_{i=\mathrm{A,B}} x_i^{\varphi}(G_i^{\circ,\varphi}(T) - H_i^{\circ,\mathrm{SER}}(298.15\ \mathrm{K})),$$

$$G^{\mathrm{id},\varphi} = RT \sum_{i=\mathrm{A,B}} x_i^{\varphi}\ \ln\ x_i^{\varphi},$$

$$G^{\mathrm{xs},\varphi} = x_{\mathrm{A}}^{\varphi} x_{\mathrm{B}}^{\varphi} L_{\mathrm{A,B}}^{\varphi},$$

where x_i^{φ} is the molar fraction of element i in the phase φ, $G^{\mathrm{ref},\varphi}$ is the reference Gibbs energy of mixing, $G^{\mathrm{id},\varphi}$ is the Gibbs energy of mixing for an ideal solution, $G^{\mathrm{xs},\varphi}$ is the excess Gibbs energy of mixing, and $L_{\mathrm{A,B}}^{\varphi}$ is the interaction parameter between A and B atoms.

The interaction parameter $L_{\mathrm{A,B}}^{\varphi}$ is generally described by a Redlich–Kister [5] polynomial:

$$L_{\mathrm{A,B}}^{\varphi} = \sum_v L_{\mathrm{A,B}}^{v,\varphi}(x_{\mathrm{A}}^{\varphi} - x_{\mathrm{B}}^{\varphi})^v. \tag{4}$$

The parameters $L_{\mathrm{A,B}}^{v,\varphi}$ can be temperature dependent:

$$L_{\mathrm{A,B}}^{v,\varphi} = a_{\mathrm{A,B}}^{v,\varphi} + b_{\mathrm{A,B}}^{v,\varphi} T + \cdots \tag{5}$$

2.4. Ordered phases

The sublattice model, developed by Temkin [6] for ionic solutions and extended later on to other types of solutions by Hillert and Staffansson [7] and Sundman and Ågren [8], is used to describe the thermodynamic properties of non-stoichiometric compounds.

The corresponding molar Gibbs energy for a compound $(\mathrm{A,B})_a(\mathrm{A,B})_b$, where A and B are the elements is given by Eq. (3) with

$$\begin{aligned} G^{\mathrm{ref},\varphi} = {} & y'_{\mathrm{A}} y''_{\mathrm{A}}(G_{\mathrm{A:A}}^{\circ,\varphi}(T) - H_{\mathrm{A}}^{\circ,\mathrm{SER}}(298.15\ \mathrm{K})) \\ & + y'_{\mathrm{A}} y''_{\mathrm{B}}(G_{\mathrm{A:B}}^{\circ,\varphi}(T) - aH_{\mathrm{A}}^{\circ,\mathrm{SER}}(298.15\ \mathrm{K}) \\ & - bH_{\mathrm{B}}^{\circ,\mathrm{SER}}(298.15\ \mathrm{K})) + y'_{\mathrm{B}} y''_{\mathrm{A}}(G_{\mathrm{B:A}}^{\circ,\varphi}(T) \\ & - aH_{\mathrm{B}}^{\circ,\mathrm{SER}}(298.15\ \mathrm{K}) - bH_{\mathrm{A}}^{\circ,\mathrm{SER}}(298.15\ \mathrm{K})) \\ & + y'_{\mathrm{B}} y''_{\mathrm{B}}(G_{\mathrm{B:B}}^{\circ,\varphi}(T) - H_{\mathrm{B}}^{\circ,\mathrm{SER}}(298.15\ \mathrm{K})), \end{aligned} \tag{6}$$

$$G^{\mathrm{id},\varphi} = RT\left(a\sum_{i=\mathrm{A,B}} y'_i\ \ln\ y'_i + b\sum_{i=\mathrm{A,B}} y''_i\ \ln\ y''_i\right), \tag{7}$$

$$\begin{aligned} G^{\mathrm{xs},\varphi} = {} & \sum_{i=\mathrm{A,B}} y'_{\mathrm{A}} y'_{\mathrm{B}} y''_i L_{\mathrm{A,B}:i}^{\varphi} + \sum_{i=\mathrm{A,B}} y''_{\mathrm{A}} y''_{\mathrm{B}} y'_i L_{i:\mathrm{A,B}}^{\varphi} \\ & + y'_{\mathrm{A}} y'_{\mathrm{B}} y''_{\mathrm{A}} y''_{B} L_{\mathrm{A,B:A,B}}^{\varphi}, \end{aligned} \tag{8}$$

where y'_i (resp. y''_i) is the site fraction of element i in the first (second) sublattice. a and b are the site fractions. $G_{i:j}^{\circ,\varphi}(T)$ is the Gibbs energy of formation of the stoichiometric compound $i_a j_b$ in the structure φ. $L_{\mathrm{A,B}:i}^{\varphi}$, (resp. $L_{i:\mathrm{A,B}}^{\varphi}$) represents the interaction term between A and B in the first (second) sublattice, the second (first) being entirely occupied by i, and $L_{\mathrm{A,B:A,B}}^{\varphi}$, the simultaneous interaction term between A and B on both sublattices.

2.5. Interstitial solutions

Interstitial solutions are also described with the sublattice model. For a binary system A–B, one of the sublattices is entirely occupied by A whereas the second contains B and vacancies denoted □: $(\mathrm{A})_a(\mathrm{B},\square)_b$. The ratio a/b is related to the crystal structure and to the type of sites occupied by B.

The molar Gibbs energy is also given by Eq. (3). However, due to the existence of vacancies in the structure a correction term is introduced to express values referred to one mole of alloy and not to one mole of sites. $G^{\mathrm{ref},\varphi}$, $G^{\mathrm{id},\varphi}$ and $G^{\mathrm{xs},\varphi}$ are now expressed as

$$G^{\mathrm{ref},\varphi} = \frac{1}{a+by''_B}\left[y''_{\square}\left(G^{\circ,\varphi}_{\mathrm{A}:\square}(T) - aH^{\circ,\mathrm{SER}}_{\mathrm{A}}(298.15\ \mathrm{K})\right) + y''_{\mathrm{B}}\left(G^{\circ,\varphi}_{\mathrm{A:B}}(T) - aH^{\circ,\mathrm{SER}}_{\mathrm{A}}(298.15\ \mathrm{K}) - bH^{\circ,\mathrm{SER}}_{\mathrm{B}}(298.15\ \mathrm{K})\right)\right], \quad (9)$$

$$G^{\mathrm{id},\varphi} = \frac{b}{a+by''_{\mathrm{B}}} RT \sum_{i=\mathrm{B},\square} y''_i \ \ln\ y''_i, \quad (10)$$

$$G^{\mathrm{xs},\varphi} = \frac{y''_B y''_{\square}}{a+by''_{\mathrm{B}}} \quad L^{\varphi}_{\mathrm{A:B},\square}. \quad (11)$$

2.6. Liquid phase

For metallic liquid solutions, the Redlich–Kister polynomial is used to describe the excess molar Gibbs energy.

When one of the elements is not metallic, the associated model (A, B, A_iB_j, ...) [9–11] and the ionic liquid model [12] $(A^{+v_A},\ldots)_P(B^{-v_B},\ldots,\square-Q,\ldots,A_iB_j,\ldots)_Q$ can both be used to describe the thermodynamic properties of the phase. Both models are present in the database. They are mathematically equivalent for binary systems.

The associate model defines as ideal reference a random mixture of atoms and associated species. The ionic solution model defines two sublattices, one occupied by cations, the second occupied by anions, vacancies charged negatively $\square^{-Q}$ and neutral species. The random mixing in each of the sublattices defines the ideal reference state of the ionic model.

In the case of a binary system A–B where no associate is considered, the associate model (A, B) is mathematically identical to the substitution solution model given by Eqs. (2)–(5). It is also equivalent to the ionic solution model if two cations of the elements are in the first sublattice and only negative charged vacancies in the second: $(A^{+v_A},B^{+v_B})_P(\square^{-Q})_Q$ with $P=Q=v_Ay_{A^{+v_A}}+v_By_{B^{+v_B}}$.

For the particular case of a binary system where a single associate is defined, the associate model (A, AO, O) is equivalent to the ionic solution model $(A^{+2})_P(O^{-2}, O, \square^{-2})_Q$ with $Q=2$ and $P=2y_{\square^{-2}}+2y_{O^{-2}}$. If two associates, AO and AO_2, are considered in the solution, the associate model (A, AO, AO_2, O) is equivalent to the ionic solution model $(A^{+2})_P(O^{-2}, AO_2, O, \square^{-2})_Q$ with $Q=2P=2y_{\square^{-2}}+2y_{O^{-2}}$. This description allows a distinction between the different levels of oxidation of the same element. A description where the two oxidation states would exist in the first sub-lattice could also be considered but for more complex systems, Hallstedt et al. [13] showed that the description $(Fe^{+2})_P(\square^{-2}, O^{-2}, FeO_{1.5})_Q$, with $Q=2$ and $P=2y_{\square^{-2}}+2y_{O^{-2}}$, was better than $(Fe^{+2}, Fe^{+3})_P(\square^{-Q}, O^{-2})_Q$, with $P=2y_{Fe^{+2}}+3y_{Fe^{+3}}$ and $P=2y_{\square^{-2}}+2y_{O^{-2}}$.

3. Zircobase

The thermodynamic database Zircobase developed in this study is issued in a format compatible with the Thermo-Calc software [14]. At present, it contains the description of all the phases of the following binary systems:

Cr–Zr [15]	Cr–Nb [16]	Fe–Nb [17]
Fe–Sn [18]	Fe–Zr [19]	H–Nb [20]
H–Zr	Nb–O [20]	Nb–Sn [22]
Nb–Zr [23]	Ni–Zr [24,25]	O–Sn [20]
O–Zr [26,21]	Sn–Zr	V–Zr [20]

As typical examples, the thermodynamic assessment of the systems Sn–Zr and H–Zr are presented hereunder.

3.1. System Sn–Zr

The phase diagram of this system is constituted by the substitution solutions in the two forms of zirconium, (α) of hcp structure and (β) of bcc structure, and three compounds $SnZr_4$, Sn_3Zr_5, Sn_2Zr. No experimental data relative to Sn-rich solid solutions are reported. The equilibria with the liquid phase are uncertain over the entire range of composition.

This system has been critically assessed by Abriata et al. [27]. Three main studies concerning this system [28–30] are available. McPherson and Hanson [28] used metallography to analyse alloys over the entire composition range. Arias et al. [29] used different techniques to determine the phase boundaries on the Zr-rich side. Speich et al. [30] determined the solubility of Sn in α-Zr by X ray analysis and strain ageing.

The stoichiometry of the compound $SnZr_4$ is mainly supported by McPherson's study [28]. Nevertheless, the full occupancy of the sites of its crystallographic structure, A15, corresponds to the stoichiometry $SnZr_3$. Kwon and Corbett [31] suggest that this compound presents a superstructure of the A15 structure initially found. But this structure was not determined. Experimental study would be needed to clarify this point. In the present study, the stoichiometry $SnZr_4$ is used.

Different forms of Sn_3Zr_5 (Sn_3Zr_5, Sn_3Zr_4 and $Sn_{3-x}Zr_5$), closely related crystallographically, were found by Kwon and Corbett [31]. They also present a phase diagram which exhibits a two phase field Sn_3Zr_5+Sn_3Zr_4 at low temperatures and a single phase

$Sn_{3-x}Zr_5$ at high temperatures. A single line separate the two fields; no eutectoid or peritectoid reaction is proposed between these three phases. This line could represent a second order reaction. Such a reaction involving two ordered phases and a disordered one has never been shown; further experiment are thus required to clarify these discrepancies. For the present study, only one phase with the stoichiometry Sn_3Zr_5 is modelled.

Partial pressures of tin derived by a model of diffusion applied to concentration profile in samples annealed between 1600 and 1970 K were presented by Zee et al. [32]. If these data were used in the optimisation procedure, the calculated phase diagram would be largely modified on the Sn-rich side. Moreover, [32] has found the same partial pressure for two compositions ($Zr_{97}Sn_3$ and $Zr_{95}Sn_5$) but different values result from the optimisation procedure. The approach of [32] does not seem to be able to evaluate accurately the partial pressure of tin in this system. These data have thus not been used in the final optimisation. The values finally calculated are lower by two orders of magnitude than [32] values.

Inconsistent values of the partial enthalpy of Zr in the Sn-rich liquid phase were reported by Valishev et al. [33] and Sudavtsova et al. [34]. Only Sudavtsova's data were found consistent with the phase diagram.

In two recent publications, Korb et al. [35] and Subasic [36] presented their results of a thermodynamic assessment of that system. In both cases, the stability of the substitutional phases, liquid, bcc–A2 and hcp–A3 increases with temperatures at $x_{Sn} = 0.5$ as shown by the values of the parameters of the excess Gibbs energies. Such a stability with increasing temperature seems unlikely. The present assessment, performed independently, does not present this unusual behaviour as the excess entropy for the liquid phase is taken equal to zero due to the lack of information.

The liquid phase and the substitutional solution were modelled with a sub-regular excess Gibbs energy of mixing. The Gibbs energy of formation of the compounds was modelled as follows:

$$G^0_{Sn_aZr_b}(T) = A_{Sn_aZr_b} + B_{Sn_aZr_b}T + aG^{A5}_{Sn}(T) + bG^{A3}_{Zr}(T), \quad (12)$$

where $A_{Sn_aZr_b}$ and $B_{Sn_aZr_b}$ are assessed and $G^{A5}_{Sn}(T)$ and $G^{A3}_{Zr}(T)$ are taken from the SGTE database [4].

The calculated phase diagram is presented in Fig. 1 together with those derived from Korb et al. [35] and Subasic [36] assessments, and the diagram in the Zr-rich corner in Fig. 2 together with the experimental data. In general, a satisfactory agreement exists as shown in Fig. 2.

3.2. System H–Zr

The binary system H–Zr has been critically assessed by Zuzek et al. [37] from the point of view of the phase

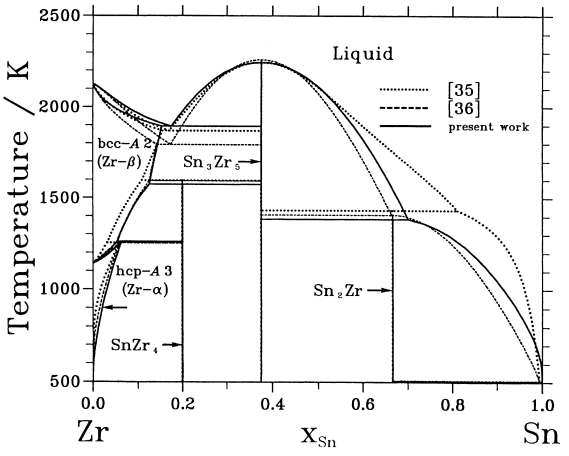

Fig. 1. Calculated phase diagram of the binary Sn–Zr system.

diagram as well as for the thermodynamic properties. Wang and Orlander [38] use Sieverts' law and the quasi-chemical model to describe the thermodynamics of this system. The present assessment has used the sublattice model to describe the thermodynamic properties of each constituting phases. The experimental data used are mainly those reported by Zuzek [37]. The main experimental features concerning this system will be presented hereunder but Zuzek's publication [37] is recommended for more details.

The different phases in the system H–Zr system are the following:

- α, the interstitial solution of H in the low temperature hcp–A3 structure of Zr,
- β, the interstitial solution of H in the high temperature bcc–A2 structure of Zr,
- δ, the hypo-stoichiometric hydride fcc–C1,
- ϵ, the fct hydride.

The phase diagram of this system presents an eutectoid reaction involving α, β and δ. The phase fields are well-known for the low hydrogen level. The large uncertainty for higher hydrogen levels can be explained by the experimental difficulties in this field but also by the impurities present in the different materials used. No experimental data involving the liquid phase are available.

Most of the experimental data concerning the phase boundaries are derived from isothermal pressure measurements [39–44,47,48,50,51,53–55,57,63]; they are thus primarily thermodynamic data and have been used as such in the optimisation procedure.

In the interstitial solution α and β, the atoms of hydrogen occupy tetrahedral sites. To model the thermodynamic properties of these two phases, the sublattice model $Zr_a(H,\Box)_b$ was used. For these two phases, the interstitial site is mainly occupied by vacancies (□). The value of the ratio b/a was obtained assuming that, for

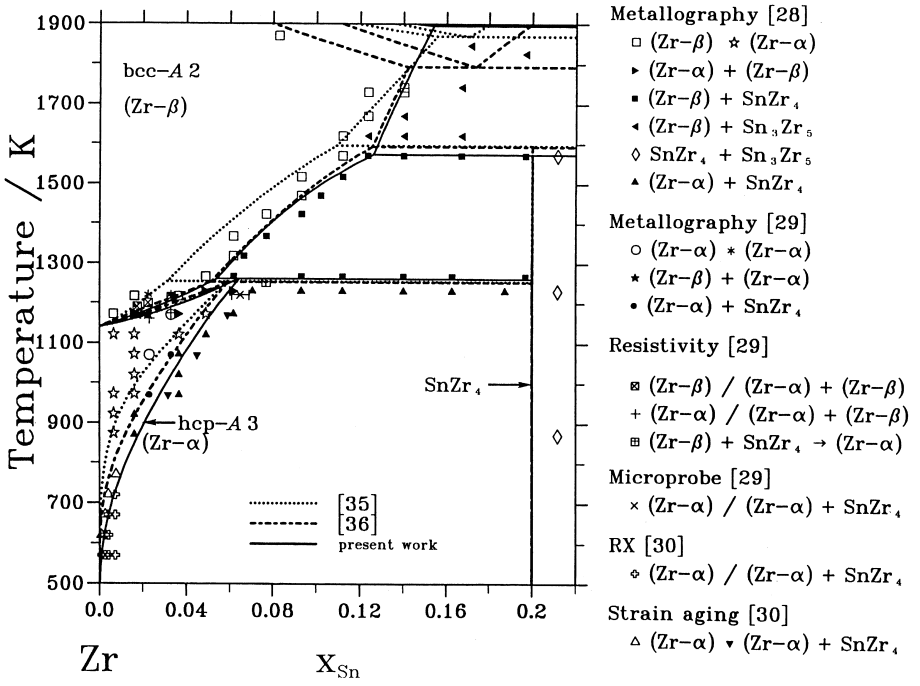

Fig. 2. Zr-rich range of the binary Sn–Zr system.

sterical reason, only half of the tetrahedral could be occupied. It is thus equal to 1 for α and 3 for β. This modelling defines two hypothetical compounds: ZrH in the A3 structure and ZrH_3 in the A2 structure. The Gibbs energies of formation of these compounds were assessed in the optimisation procedure as functions of the type

$$G^{\varphi}_{ZrH_{b/a}}(T) = A^{\varphi}_{ZrH_{b/a}} + B^{\varphi}_{ZrH_{b/a}}T + G^{\varphi}_{Zr}(T) + \frac{b}{a}G^{gas}_{\frac{1}{2}H_2}(T) \tag{13}$$

while the lattice stability of the pure Zr in these structures, $G^{\varphi}_{Zr}(T)$ and $G^{gas}_{1/2\,H_2}$, were taken from [4]. No excess interaction term was introduced for the A3 phase while a sub-regular excess parameter was needed for the A2 phase.

The two hydrides were described with the sublattice model $Zr(H,\Box)_2$ where the second sublattice is mainly occupied by hydrogen. The lattice stability of the pure zirconium in the fcc–C1 structure was taken equal to the one in the fcc–A1 structure [4]. The lattice stability of the pure zirconium in the structure of fct hydride was assumed slightly more positive, differing by +1 kJ mol^{-1} compared to the fcc one. The Gibbs energies of formation of the stoichiometric hydrides were assessed as functions of the following type:

$$G^{\varphi}_{ZrH_2} = A^{\varphi}_{ZrH_2} + B^{\varphi}_{ZrH_2}T + C^{\varphi}_{ZrH_2}T\ln T + G^{A3}_{Zr}(T) + 2G^{gas}_{\frac{1}{2}H_2}(T). \tag{14}$$

A regular excess Gibbs energy was used for the fct phase ϵ and a sub-regular for the fcc–C1.

The gas phase was described as an ideal mixture of H, H_2, Zr, Zr_2 and HZr. No solubility of hydrogen was modelled in the liquid phase. None of the thermodynamic parameters needed for these two phases were assessed in the present study; they were taken from the SGTE database [70].

An initial optimisation was done using phase diagram information and thermodynamic data for the hydride phases. This first step, using a reduced number of experimental points allow a quick estimation of the thermodynamic parameters describing the different phases of the system. Experimental pressures for different temperatures and compositions were then introduced for a more accurate assessment.

The assessed parameters in the present study are presented in Appendix A. The entire calculated phase diagram and the solubility of H in (α) are compared with experimental data in Figs. 3 and 4. There is a satisfactory agreement between the calculated and experimental results. Several isothermal calculated pressures versus composition are compared with experimental data in Fig. 5. A satisfactory agreement is obtained also for the different sets of data. It has to be noticed that the calculated curves are in fairly good agreement with the more recent data [67,68] obtained with zirconium of high purity but on restricted ranges of temperature and composition.

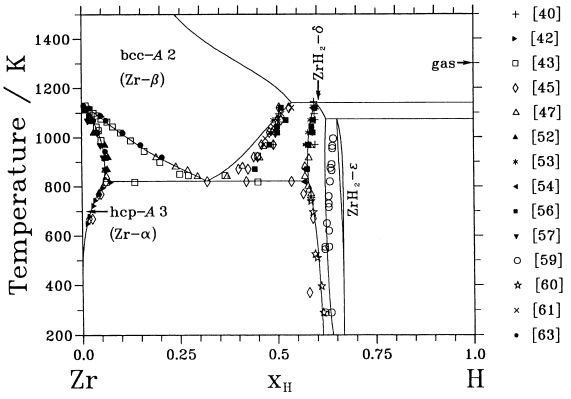

Fig. 3. Calculated phase diagram of the binary H–Zr system [40,42,43,45,47,52–54,56–61,63].

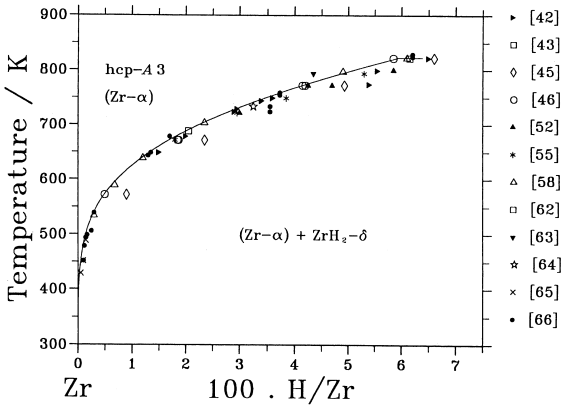

Fig. 4. Calculated solubility of hydrogen in α-zirconium [42,43,45,46,52,55,58,62–66].

4. Thermodynamic predictions of α/β transformation temperatures on industrial alloys:

The current thermodynamic database enables some extrapolations on ternary and higher order systems. For example, it is of technological interest to be able to estimate the α/β phase transformation temperatures as a function of the chemical composition of typical industrial alloys because these transformations occur during fabrication routes, during welding operations and/or during accidental thermal transients i.e. 'Loss of Coolant Accidents'.

Fig. 6 shows the comparison of experimental data with thermodynamic predictions from the ternary Zr–Nb–O system on two Zr–Nb industrial alloys (i.e. Zr–1% Nb and Zr–2.5% Nb alloys). The experimental procedure used to derive the phase fractions of β as a function of the temperature in quasi-equilibrium conditions is detailed in Ref. [69]. This experimental procedure is mainly based on the use of high temperature–high

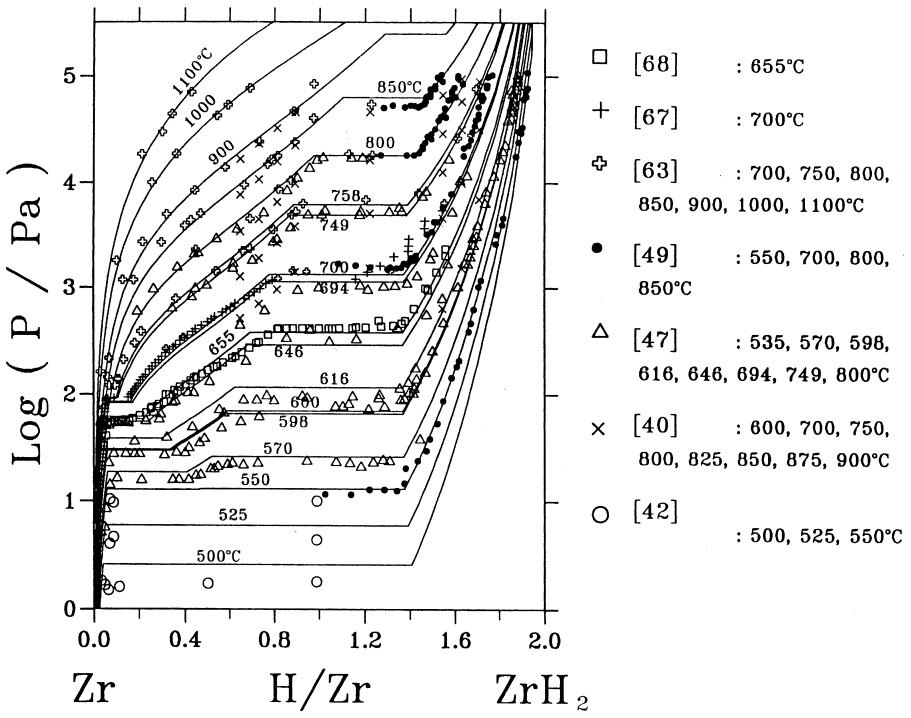

Fig. 5. Pressure–composition–temperature diagram of the binary system H–Zr [40,42,47,49,63,67,68].

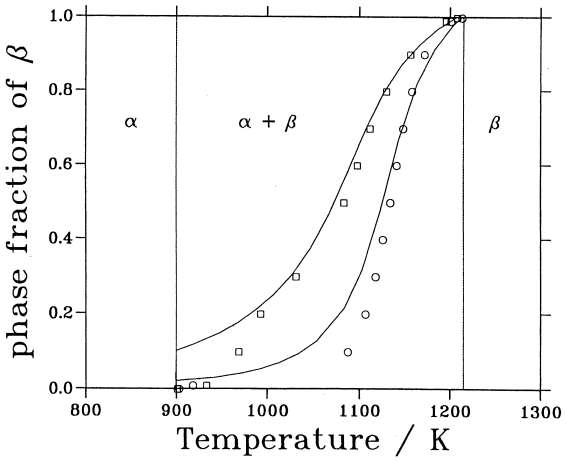

Fig. 6. β phase fraction as a function of temperature in equilibrium conditions for Zr–1% Nb (○) and Zr–2.5% Nb (□) alloys for a typical oxygen content of 1200 wt ppm.

sensitivity calorimetry performed at different heating/cooling rates ranging from 1 to 10°/min. From this figure, it appears that the extrapolation of the thermodynamic calculations using the Zircobase for the Zr–Nb–O system gives fairly accurate predictions of the β phase fractions vs. temperature. It should be noticed that the same calculations have been made considering only the binary Zr–Nb system. In this last case, the (α + β)/β temperature is strongly under-estimated, showing the necessity to take into account the α-stabilizing effect of oxygen on α/β temperatures of industrial alloys, for accurate thermodynamic predictions.

Fig. 7 shows the comparison of some experimental and calculated α/β phase transformation temperatures of different experimental low-Sn Zy4 alloys with oxygen contents ranging from 100 up to 4000 wt ppm. Thermodynamic calculations have been performed considering the Zr–1.2% Sn–0.2% Fe–0.1% Cr basic chemical composition of the alloys with different amounts of oxygen. The temperatures corresponding to 50% α/50% β alloys are shown in Fig. 7 because they correspond to the higher accuracy of the calorimetric measurements. Due to that accuracy, the experimental temperatures for α/(α + β) alloys $T_{(\alpha/(\alpha+\beta))}$ and those for (α + β)/β alloys $T_{((\alpha+\beta)/\beta)}$ correspond to a few percent of α and β phases. So it is not surprising that these last experimental values are respectively slightly above or below the calculated $T_{(\alpha/(\alpha+\beta))}$ and $T_{((\alpha+\beta)/\beta)}$. Again, the strong α-stabilizing effect of oxygen is noticeable and the thermodynamic predictions are in fairly good agreement with the experimental data.

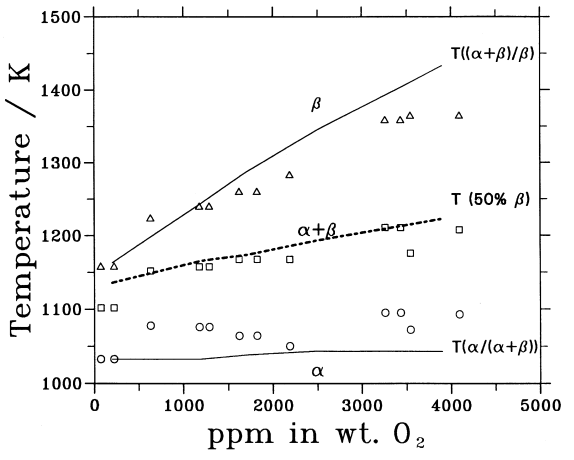

Fig. 7. α/β transformation temperatures as a function of oxygen content for low tin (1.2% Sn) Zy4 alloys.

5. Conclusions

Zircobase, a thermodynamic database has been developed for zirconium alloys. Data for 15 binary systems were either assessed in this study or extracted from the literature. This database is open for further developments and can be used for extrapolations of higher order systems.

Preliminary thermodynamic calculations of α/β temperatures on ternary and higher order systems show a fairly good agreement with some experimental data obtained on industrial Zr–Nb and Zy4 type alloys with different oxygen contents.

Acknowledgements

Special thanks are given to EDF and Framatome, the French utility and fuel designer and supplier, as well as the French Safety Authorities for their interest and financial support for this work. Specific mentions are given to Pierre Barberis, CEZUS, for his stimulating discussions during the course of this work.

Appendix A. Thermodynamic properties of the solution and compound phases (J mol^{-1})

System Sn–Zr

Phase liquid

$$L^{0,\text{liquid}}_{\text{Sn,Zr}} = -172881,$$

$$L^{1,\text{liquid}}_{\text{Sn,Zr}} = -1108.$$

Phase bcc–A2

$$L^{0,\text{bcc–A2}}_{\text{Sn,Zr:}\square} = -203172 + 9.9\ T,$$

$$L^{1,\mathrm{bcc-A2}}_{\mathrm{Sn,Zr:}\square} = 54720 - 37.58\ T.$$

Phase hcp–A3

$$L^{0,\mathrm{hcp-A3}}_{\mathrm{Sn,Zr:}\square:\square} = -238817 + 31.61\ T,$$

$$L^{1,\mathrm{hcp-A3}}_{\mathrm{Sn,Zr:}\square:\square} = 7403.$$

Phase $SnZr_4$

$$G^{\circ}_{\mathrm{SnZr_4}}(T) - H^{\circ,\mathrm{bct-A5}}_{\mathrm{Sn}}(298.15\ \mathrm{K}) - 4\ H^{\circ,\mathrm{hcp-A3}}_{\mathrm{Zr}}(298.15\ \mathrm{K}) = -294493 + 62.42\ T + \mathrm{GHSER_{Sn}} + 4\ \mathrm{GHSER_{Zr}}.$$

Phase Sn_3Zr_5

$$G^{\circ}_{\mathrm{Sn_3Zr_5}}(T) - 3H^{\circ,\mathrm{bct-A5}}_{\mathrm{Sn}}(298.15\ \mathrm{K}) - 5\ H^{\circ,\mathrm{hcp-A3}}_{\mathrm{Zr}}(298.15\ \mathrm{K}) = -652414 + 65.44\ T + 3\ \mathrm{GHSER_{Sn}} + 5\ \mathrm{GHSER_{Zr}}.$$

Phase Sn_2Zr

$$G^{\circ}_{\mathrm{Sn_2Zr}}(T) - 2H^{\circ,\mathrm{bct-A5}}_{\mathrm{Sn}}(298.15\ \mathrm{K}) - H^{\circ,\mathrm{hcp-A3}}_{\mathrm{Zr}}(298.15\ \mathrm{K}) = -220180 + 45.61\ T + 2\ \mathrm{GHSER_{Sn}} + \mathrm{GHSER_{Zr}}.$$

System H–Zr

Phase bcc–A2

$$G^{\circ,\mathrm{bcc-A2}}(T) - H^{\circ,\mathrm{hcp-A3}}_{\mathrm{Zr}}(298.15\ \mathrm{K}) - 3\ H^{\circ,\mathrm{gas}}_{\frac{1}{2}\mathrm{H_2}}(298.15\ \mathrm{K}) = 44853 + \mathrm{GHSER_{Zr}} + 3\ \mathrm{GHSER_H},$$

$$L^{0,\mathrm{bcc-A2}}_{\mathrm{Zr:H,}\square} = -474971 + 359\ T,$$

$$L^{1,\mathrm{bcc-A2}}_{\mathrm{Zr:H,}\square} = -267893 + 200\ T.$$

Phase hcp–A3

$$G^{\circ,\mathrm{hcp-A3}}(T) - H^{\circ,\mathrm{hcp-A3}}_{\mathrm{Zr}}(298.15\ \mathrm{K}) - H^{\circ,\mathrm{gas}}_{\frac{1}{2}\mathrm{H_2}}(298.15\ \mathrm{K}) = -45965 + 41.6\ T + \mathrm{GHSER_{Zr}} + \mathrm{GHSER_H}.$$

Phase fcc–C1

$$G^{\circ,\mathrm{fcc-C1}}(T) - H^{\circ,\mathrm{hcp-A3}}_{\mathrm{Zr}}(298.15\ \mathrm{K}) - 2\ H^{\circ,\mathrm{gas}}_{\frac{1}{2}\mathrm{H_2}}(298.15\ \mathrm{K}) = -170490 + 208.2\ T - 9.47\ T\ \ln(T) + \mathrm{GHSER_{Zr}} + 2\ \mathrm{GHSER_H},$$

$$L^{0,\mathrm{fcc-C1}}_{\mathrm{Zr:H,}\square} = 14385 - 6.0\ T,$$

$$L^{1,\mathrm{fcc-C1}}_{\mathrm{Zr:H,}\square} = -106445 + 87.3\ T.$$

Phase ZrH_2–ϵ

$$G^{\circ,\mathrm{ZrH_2-\epsilon}}(T) - H^{\circ,\mathrm{hcp-A3}}_{\mathrm{Zr}}(298.15\ \mathrm{K}) - 2\ H^{\circ,\mathrm{gas}}_{\frac{1}{2}\mathrm{H_2}}(298.15\ \mathrm{K}) = -168215 + 110.5\ T + 3.866\ T\ \ln T + \mathrm{GHSER_{Zr}} + 2\ \mathrm{GHSER_H},$$

$$L^{0,\mathrm{ZrH_2-\epsilon}}_{\mathrm{Zr:H,}\square} = 19900.$$

References

[1] J.P. Mardon, G. Garner, P. Beslu, D. Charquet, Update on the development of advanced zirconium alloys for PWR fuel rod claddings, in: ANS International Topical Meeting of Light Water Reactor Fuel Performance, Portland, OR, USA, 2–6 March 1997, pp. 405–412.
[2] B. Cox, V.G. Kritsky, C. Lemaignan, V. Polley, I.G. Richtie, H. Ruhmann, V.N. Sishov, Waterside Corrosion of Zirconium Alloys in Nuclear Power Plants, IAEA TECDOC 996, January 1998, Vienna, Austria.
[3] C. Lemaignan, A.T. Motta, in: R.W. Cahn, P. Haasen, E.J. Kramer (Eds.), Zirconium Alloys in Nuclear Applications, Materials Science and Technology, vol. 10B, Nuclear Materials, VCH, Weinheim, 1994, p. 1.
[4] A. Dinsdale, Calphad 15 (1991) 317.
[5] O. Redlich, A. Kister, Ind. Eng. Chem. 40 (1948) 345.
[6] M. Temkin, Acta Phys. Chim. 20 (1945) 411.
[7] M. Hillert, L.I. Staffanson, Acta Chem. Scand. 24 (1970) 3618.
[8] B. Sundman, J. Ågren, J. Phys. Chem. Solids 42 (1981) 297.
[9] F. Dolezalek, Z. Phys. Chem. 64 (1908) 727.
[10] A.S. Jordan, Metall. Trans. 1 (1970) 239.
[11] F. Sommer, Z. Metallkd. 73 (1982) 72, 77.
[12] M. Hillert, B. Jansson, B. Sundman, J. Ågren, Metall. Trans. 16A (1985) 261.
[13] B. Hallstedt, M. Hillert, M. Selleby, B. Sundman, Calphad 18 (1994) 31.
[14] B. Sundman, B. Jansson, J.-O. Anderson, Calphad 2 (1985) 153.
[15] K. Zeng, M. Hämäläinen, I. Ansara, COST 507: Thermochemical Database for Light Metal Alloys, in: I. Ansara (Ed.), Publ. ECSC-EEC-EAEC, Brussels and Luxembourg, 1995, 111–114.
[16] J.G. Costa Neto, S.G. Fries, H.L. Lukas, S. Gama, G. Effenberg, Calphad 17 (1993) 219.
[17] C. Toffolon, C. Servant, Calphad, to be published.
[18] K.C. Hari Kumar, P. Wollants, L. Delaey, Calphad 20 (1996) 139.
[19] C. Servant, C. Gueneau, I. Ansara, J. Alloys Comp. 220 (1996) 19.
[20] N. Dupin, I. Ansara, to be published.
[21] N. Dupin, I. Ansara, P. Liang, H. Seifert, to be published.
[22] C. Toffolon, C. Servant, B. Sundman, J. Phase Equilibria 19 (1998) 479.
[23] A. Fernandez Guillermet, Z. Metallkd. 82 (1991) 478.
[24] N. Saunders, Calphad 9 (1985) 297.

[25] I. Ansara, N. Dupin, J.M. Joubert, M. Latroche, A. Percheron-Guégan, J. Phase Equilibria 19 (1998) 6.
[26] P. Liang, S.G. Fries, H.L. Lukas, H.J. Seifert, F. Aldinger, G. Effenberg, private communication.
[27] J.P. Abriata, J.C. Bolcich, D. Arias, Bull. Alloy Phase Diagrams 4 (1983) 147.
[28] D.J. McPherson, M. Hanson, Trans. ASM 45 (1953) 915.
[29] D. Arias, unpublished work, ASM APD-R-83-003, quoted by [27].
[30] G.R. Speich, S.A. Kulin, Zirconium and Zirconium Alloys, Am. Soc. Metals 197 (1953) cited by [27].
[31] Y.U. Kwon, J.D. Corbett, Chem. Mater. 2 (1990) 27.
[32] R.H. Zee, J.F. Watters, R.D. Davidson, Phys. Rev. B 34 (1986) 6895.
[33] M.G. Valishev, O.Yu. Sidorov, S.P. Koleshnikov, P.V. Geld, Izvest. Akad. Nauk. Metally 4 (1992) 47.
[34] V.S. Sudavtsova, G.I. Batalin, Rasplavy 1 (1990) 88.
[35] J. Korb, K. Hack, Thermochemical Database for Light Alloys, vol. 2, p. 290, I. Ansara, A. Dinsdale, M.H. Rand (Eds.), 1998, Eur 18499 EN.
[36] N. Subasic, Calphad 22 (1998) 157.
[37] E. Zuzek, J.P. Abriata, A. San-Martin, F.D. Manchester, Metall. Trans. A 24A (1993) 1993.
[38] W.-E. Wang, D.R. Olander, J. Am. Ceram. Soc. 78 (1995) 3323.
[39] A. Gulbransen, K.F. Andrew, J. Electrochem. Soc. 101 (1954) 474.
[40] R.K. Edwards, P. Levesque, D. Cubicciotti, J. Am. Chem. Soc. 77 (1955) 1307.
[41] P. Gilbert, USAEC Rep. NAA-SR-1026 (1955) cited by [62].
[42] A. Gulbransen, K.F. Andrew, Trans. AIME 203 (1955) 136.
[43] C.E. Ells, A.D. McQuillan, J. Inst. Met. 85 (1956) 89.
[44] M.W. Mallet, W.M. Albrecht, J. Electrochem. Soc. 104 (1957) 142.
[45] T.M. Douglas, J. Am. Chem. Soc. 80 (1958) 5040.
[46] L. Espagno, P. Azou, P. Bastien, C. R. Acad. Sci. 249 (1959) 1105.
[47] L.D. Lagrange, L.J. Dykstra, J.M. Dixon, U. Merten, J. Phys. Chem. 63 (1959) 2035.
[48] D.F. Atkins, USAEC Rep. NAA-SR-4245 (1960).
[49] G.G. Libowitz, USAEC Rep. NAA-SR-5015, Atomics International (1960).
[50] J.R. Morton, D.S. Stark, Trans. Farad. Soc. 56 (1960) 351.
[51] V.V. Sofina, N.G. Pavlovskaya, Zh. Fiz. Khim. 34 (1960) 1004.
[52] N. Someno, J. Jpn. Inst. Met. 24 (1960) 249.
[53] R.L. Beck, Trans. ASM 55 (1962) 542.
[54] G.G. Libowitz, J. Nucl. Mater. 5 (1962) 228.
[55] G. Ostberg, J. Nucl. Mater. 5 (1962) 208.
[56] K.P. Singh, J.G. Parr, Trans. Faraday Soc. 59 (1963) 2256.
[57] W.H. Erickson, D. Hardie, J. Nucl. Mater. 13 (1964) 254.
[58] J.J. Kearns, J. Nucl. Mater. 22 (1967) 292.
[59] K.E. Moore, W.A. Young, J. Nucl. Mater. 27 (1968) 335.
[60] K.E. Moore, J. Nucl. Mater. 32 (1969) 46.
[61] V.K. Sinha, K.P. Singh, J. Nucl. Mater. 36 (1970) 211.
[62] D.G. Westlake, S.T. Ockers, J. Nucl. Mater. 37 (1970) 236.
[63] M. Tada, Y.C. Chuang, Chitaniumu Jirikoniumu 19 (1971) 260.
[64] G.J.C. Carpenter, J.F. Watters, J. Nucl. Mater. 73 (1978) 190.
[65] C.D. Cann, A. Atrens, J. Nucl. Mater. 88 (1980) 42.
[66] I.G. Ritchie, K.W. Sprungmann, AECL-7806, Atomic Energy of Canada Ltd., December 1983.
[67] S. Yamanaka, T. Tanaka, M. Miyake, J. Nucl. Mater. 167 (1989) 231.
[68] P. Dantzer, W. Luo, T.B. Flanagan, J.D. Clewley, Metall. Trans. A 24A (1993) 1993.
[69] T. Forgeron, J.C. Brachet, A. Castaing, F. Barcelo, J. Hivroz, J.P. Mardon, C. Bernaudat, Experiment and Modelling of Advanced Fuel Rod Cladding Behaviour under LOCA conditions, α–β Phase Transformation Kinetics and EDGAR Methodology, Proceedings of the 12th International Symposium on Zr in the Nuclear Industry, Toronto, Ontario, June 1998, ASTM-STP, to be published.
[70] I. Ansara, in: J.-P. Caliste, A. Truyof, J.H. Westbrook (Eds.), Theromodynamic Modelling and Materials Data Engineering, Springer, Berlin, 1998, p. 33.